

Charge and spin states of metal atoms adsorbed on ultrathin MgO/Fe(001) films

Jinwoo Park and B. D. Yu*

Department of Physics, University of Seoul, Seoul 130-743, Korea

Hanchul Kim

Department of Physics, Sookmyung Women's University, Seoul 140-742, Korea

(Received 22 January 2009; revised manuscript received 7 April 2009; published 25 June 2009)

Recent works on nanosized metal systems demonstrated the importance of charge states in the various reactions of metal atoms adsorbed on metal-supported ultrathin oxide films, such as MgO/Mo(001) and MgO/Ag(001). With the use of density-functional theory calculations, we propose ultrathin MgO/Fe(001) film as a viable thin oxide model system that presents a way of modifying the charge and/or spin states of metal adsorbates on surfaces. Indeed, due to the presence of the Fe substrate, Pd atoms were calculated to be charged and/or spin polarized, depending on the MgO thickness, which contrasted that of previous results with Pd/MgO/Mo(001) and Pd/MgO/Ag(001).

DOI: [10.1103/PhysRevB.79.233407](https://doi.org/10.1103/PhysRevB.79.233407)

PACS number(s): 68.43.Bc, 68.43.Fg, 82.65.+r

Ultrathin oxide films have attracted much interest due to their importance in technological applications, such as in heterogeneous catalysis, gas sensors, fuel cells, protective coatings, and electronic devices.^{1,2} In particular, metal-supported ultrathin oxide films are electrically conductive in a way that is different from insulating thicker or bulk-like oxides. This feature allows investigations with various modern experimental techniques, such as scanning tunneling microscopy (STM), scanning tunneling spectroscopy, and photoelectron spectroscopy. Thus, metal-supported ultrathin oxide films have been widely employed as model oxides for the investigations of physical and chemical properties of metal atoms or clusters on thicker or bulk-like oxides.³⁻⁵

The electronic and chemical properties of metal adsorbates have been discovered to depend on the thickness of oxide films and the metal species of substrates.³⁻⁹ The extraordinary chemical properties of metal adsorbates on ultrathin oxide films in contrast to surfaces of thicker or bulk-like oxides can be traced back to charge-transfer processes involving the coupling of the oxide films to the metal substrates. A prototypical oxide example is MgO, where well-ordered thin oxide films of finite thickness have been grown on a wide variety of metal substrates. For Au atoms adsorbed on ultrathin MgO films grown on Mo(001), the negative charging of the Au atoms was deduced from theoretical investigations.⁶ As such, metal atoms with high electron affinity (EA) and support metals with low work function were proposed as possible candidates for the efficient charging of metal atoms on ultrathin oxide films.⁶ Experimental observations for such a mechanism were obtained in recent works on Au and Pd atoms deposited on ultrathin MgO films grown on Ag(001).⁷ More recent low-temperature STM measurements¹⁰ also showed images of well-separated Au monomers for MgO/Ag(001) that were caused by the repulsive interactions between the negatively charged Au monomers. This clearly suggests the presence of negatively charged Au atoms on MgO/Ag(001).

In this work, the adsorption of metal atoms (Au and Pd) on ultrathin MgO films grown on (001) surfaces of Fe was investigated by carrying out *ab initio* calculations based on the density-functional theory (DFT).¹¹ So far, MgO has been

widely used as an oxide barrier separating two ferromagnetic materials in magnetic tunnel junctions.^{12,13} MgO films are successfully grown on Fe(001) due to their favorable physical properties, such as a small lattice mismatch and suitable surface free energies of MgO and Fe.¹⁴⁻¹⁷ Here, we propose MgO/Fe(001) as viable thin oxide model system for the study of the adsorption of metal atoms on metal-supported ultrathin oxides. Our calculations showed that negative charging of Au atoms occurs through charge transfer from Fe to Au as in the metal substrates of Mo and Ag.^{6,7,9,10} It was also found that the negative charging happens even for Pd with low EA. Interestingly, Pd atoms were spin polarized due to the charge transfer in contrast to Pd/MgO/Fe(001). Our calculations demonstrated that the Fe substrate we propose in this work presents a way of modifying the electronic and chemical properties of metal adsorbates, such as charge and spin states.

Here, all calculations were carried out using the DFT within the spin-dependent generalized gradient approximation (GGA)¹⁸ and ultrasoft pseudopotentials¹⁹ as implemented in the VASP.²⁰⁻²² To simulate the adsorption of transition-metal (TM) atoms on Fe-supported MgO(001) surfaces, we used a repeating slab structure consisting of five Fe layers with 17 Å vacuum region and a 3×3-surface unit cell. The TM adatom and the ultrathin MgO film were deposited only on one side of the slab, and the MgO film thickness was made to vary from one to five atomic layers. In the calculations, we employed an ideal, abrupt MgO/Fe(001) interface,^{14,17} where the oxygen atoms were located on top of the substrate Fe atoms and MgO[110] was parallel to Fe[100], as shown in Fig. 1. For the MgO/Fe(001) slab, we used the theoretical lattice constant of 2.87 Å of bulk bcc Fe in the GGA calculations. The cutoff energy of 260 eV and the uniform mesh of 9 k points in the surface Brillouin zone (SBZ) of the surface unit cell were used. All atoms were relaxed in the slab except for the bottom two Fe-layer atoms. The geometry optimization was stopped when the remaining forces were smaller than 0.02 eV/Å. Some test calculations were also carried out with the use of a more extensive set of parameters such as the cutoff energy of 300 eV, the 25 k points in the SBZ, the six Fe layers, and the two-sided slab

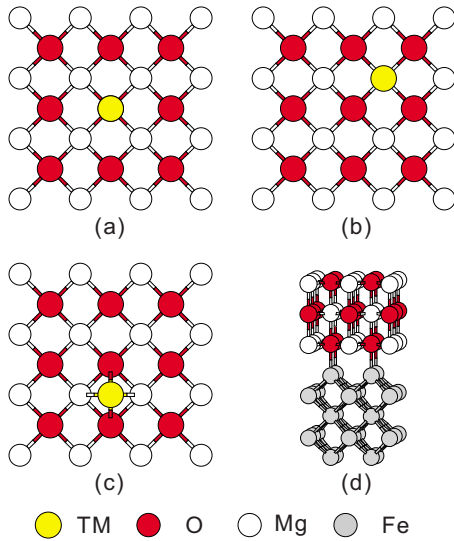


FIG. 1. (Color online) Top views of the adsorption structures of TM atoms on Fe-supported MgO(001): adsorption (a) on top of oxygen, (b) on top of magnesium, and (c) in a hollow site. The perspective view of clean MgO/Fe(001) is represented in (d).

geometry of MgO/Fe(001). These tests suggest that the calculated adsorption energies and the energy differences are accurate up to 0.04 and 0.01 eV, respectively, when employing the above calculation parameters. The computational accuracy is sufficient for the purpose of our study.

To study the adsorption of the TM atoms (Au and Pd) on the ultrathin MgO/Fe(001) surface, three possible adsorption sites were considered: adsorption on top of a surface oxygen anion, on top of a surface magnesium cation, and in a surface hollow site (see Fig. 1). The adsorption-energy E_{ads} was calculated as the difference of total energies. Here, $E_{\text{ads}} = E_{\text{TM/MgO/Fe(001)}} - E_{\text{MgO/Fe(001)}} - E_{\text{TM}}$, where $E_{\text{TM/MgO/Fe(001)}}$ and $E_{\text{MgO/Fe(001)}}$ are the total energies of the TM-adsorbed and clean MgO/Fe(001) surfaces, respectively. E_{TM} is the total energy of a spin-polarized free TM atom. The calculated structural parameters and adsorption energies are summarized in Table I. Figure 2 shows the calculated adsorption energies of the Au and the Pd atoms at the various adsorption

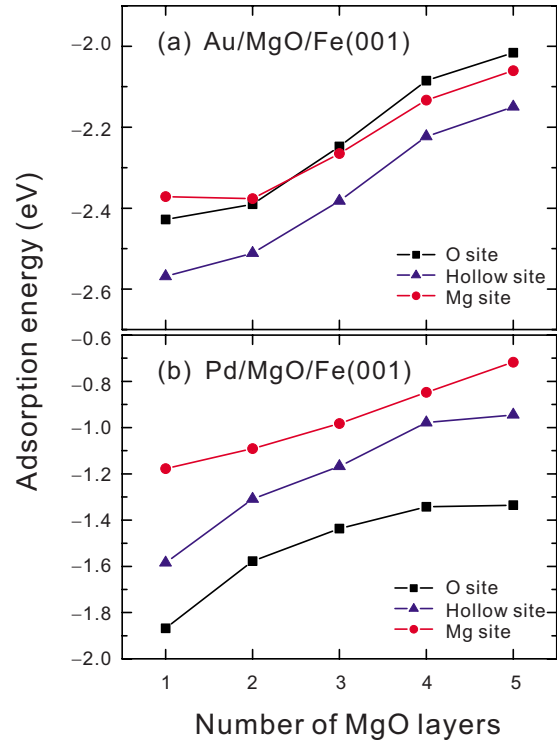


FIG. 2. (Color online) Adsorption energies of Au and Pd at the various adsorption sites on MgO/Fe(001) as a function of the number of MgO layers.

sites on MgO/Fe(001) as a function of the number of MgO layers. Moreover, the adsorption behavior of the reduced binding with increasing MgO thickness was obtained for gold, which turned out to be similar to the adsorption on MgO/Mo(001).^{6,9} As for the stable adsorption site, Au atoms favorably adsorb on the hollow site of MgO/Fe(001). The hollow site was more stable by 0.09–0.20 eV than the other adsorption sites as shown in Table I. This is in contrast to that of the unsupported MgO(001) films, where TM atoms generally favor the position on top of a surface oxygen atom.²³ In addition, for the 3–5 MgO layers on Fe(001), the Mg site showed intermediate values in the adsorption ener-

TABLE I. Calculated results of TM atoms adsorbed at the three different sites on MgO/Fe(001) and MgO(001). nL , d , and E_{ads} represent the number of MgO layers, the interatomic distance, and the adsorption energy of TM, respectively.

nL	Au			Pd		
	O $E_{\text{ads}}(d_{\text{Au-O}})$ eV (Å)	Mg $E_{\text{ads}}(d_{\text{Au-Mg}})$ eV (Å)	Hollow $E_{\text{ads}}(d_{\text{Au-Mg}}, d_{\text{Au-O}})$ eV (Å)	O $E_{\text{ads}}(d_{\text{Pd-O}})$ eV (Å)	Mg $E_{\text{ads}}(d_{\text{Pd-Mg}})$ eV (Å)	Hollow $E_{\text{ads}}(d_{\text{Pd-Mg}}, d_{\text{Pd-O}})$ eV (Å)
1	-2.43 (2.79)	-2.37 (2.58)	-2.57 (2.76, 3.19)	-1.87 (2.66)	-1.18 (2.51)	-1.58 (2.62, 3.14)
2	-2.39 (2.85)	-2.38 (2.58)	-2.51 (2.78, 3.23)	-1.58 (2.33)	-1.09 (2.54)	-1.31 (2.67, 3.13)
3	-2.25 (2.84)	-2.26 (2.59)	-2.38 (2.79, 3.23)	-1.43 (2.26)	-0.98 (2.55)	-1.17 (2.69, 3.08)
4	-2.08 (2.85)	-2.13 (2.59)	-2.22 (2.80, 3.22)	-1.34 (2.20)	-0.85 (2.59)	-0.98 (2.67, 2.79)
5	-2.02 (2.85)	-2.06 (2.59)	-2.15 (2.80, 3.22)	-1.34 (2.17)	-0.72 (2.60)	-0.94 (2.68, 2.77)
5 ^a	-0.79 (2.33)	-0.42 (2.76)	-0.58 (2.88, 2.86)	-1.23 (2.12)	-0.51 (2.60)	-0.87 (2.65, 2.58)
5 ^b	-0.91 (2.29)	-0.49 (2.75)	-0.69 (2.84, 2.81)	-1.40 (2.09)	-0.58 (2.57)	-1.05 (2.61, 2.53)

^aUnsupported 5ML MgO films with the surface lattice constant of Fe(001).

^bUnsupported 5ML MgO films with the surface lattice constant of MgO(001).

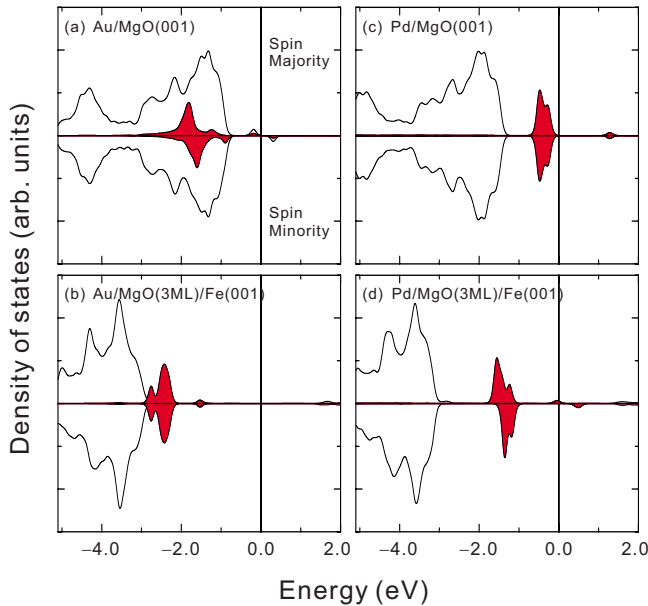


FIG. 3. (Color online) Densities of states (DOS) projected on the TM atom (shaded) and the O atoms (solid lines) in the top two MgO layers for the adsorption of Au and Pd at the various adsorption sites: (a) Au at the hollow site on MgO(001), (b) Au at the hollow site on MgO(3ML)/Fe(001), (c) Pd at the O site on MgO(001), and (d) Pd at the O site on MgO(3ML)/Fe(001). The energy zero is set at the Fermi energy E_F . In (a)–(d), the vacuum levels are located at 5.12, 4.02, 4.35, and 3.66 eV, respectively.

gies. A more detailed investigation of the Au adsorption showed that the Au adatom diffuses on MgO/Fe(001) along the channel through the Mg site. As such, the surface diffusion barrier was determined by the energy difference between the hollow and the Mg sites and the calculated diffusion barriers were found to be very low, ranging from 0.09 to 0.12 eV.

To understand the detailed role of the Fe support in the adsorption of Au on MgO/Fe(001), the electronic structures of Au/MgO(3ML)/Fe(001) and Au/MgO(001) with the adsorption of Au at the hollow site were investigated by analyzing the projected spin-polarized density of states for each atom. For Au at the hollow site on MgO(001), the spin-polarized half-filled $6s$ -derived states of Au were formed in the gap region. The Fermi energy lay 0.7 eV above the top of the O valence band and the split-off energy of the Au $6s$ -derived states near the Fermi energy was 0.5 eV [see Fig. 3(a)]. For Au adsorbed at the hollow site on MgO/Fe(001), however, a different behavior was obtained: the Fermi energy lay 2.9 eV above the top of the O valence band and therefore the empty part of the Au $6s$ -derived states shifted below the Fermi energy [see Fig. 3(b)]. The Au $6s$ -derived states were formed 1.5 eV below the Fermi energy. As such, the charge transfer to the Au atom to form negatively charged Au happened less costly than that with the others.

Figure 4(a) shows the isosurface plot of the electron-density difference $\Delta\rho$ for Au/MgO(3ML)/Fe(001); $\Delta\rho = \rho_{\text{TM/MgO/Fe}} - \rho_{\text{TM}} - \rho_{\text{MgO}} - \rho_{\text{Fe}}$. Substantial accumulation of electrons was obtained around Au [see Fig. 4(a)]. Together

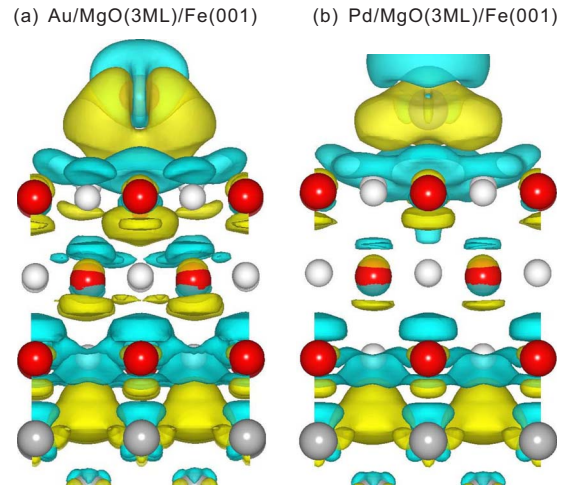


FIG. 4. (Color online) Isosurface plots of electron-density difference $\Delta\rho$ with the side view of the adsorption structures for (a) Au at the hollow site on MgO(3ML)/Fe(001) and (b) Pd at the O site on MgO(3ML)/Fe(001); $\Delta\rho = \rho_{\text{TM/MgO/Fe}} - \rho_{\text{TM}} - \rho_{\text{MgO}} - \rho_{\text{Fe}}$. Electron accumulation and depletion regions are represented by light gray (yellow) and dark gray (blue), respectively. The isosurface levels are ± 0.0014 electrons/bohr³.

with the electron accumulation, polarization was also induced all the way from the MgO/Fe interface to the Au atom, including the oxide region [see Fig. 4(a)]. Here, it is noted that, once the charge transfer and the polarization induction occur, interactions between the negatively charged Au and the ionic oxide atoms become ionic. The ionic interactions are much stronger than those between the charge-neutral Au and the oxide atoms of MgO(001). The ionic nature of the interactions is well reflected in the shorter interatomic distances of Au with the neighboring cation atoms compared with those of Au on MgO(001) (see Table I). For instance, the interatomic distance $d_{\text{Au-Mg}}$ for Au at the hollow site on MgO(3ML)/Fe(001) was shorter by ~ 0.1 Å than that for Au at the hollow site on unsupported MgO(001). The differences in $d_{\text{Au-Mg}}$ for the Mg adsorption site were more significant. This indicates that the strong ionic interactions are always actuated between the charged Au and the oxide atoms whenever the charge transfer and the polarization induction happen. This further explains well the larger adsorption energies of Au for Au/MgO/Fe(001) with thicker 3–5 MgO films.

The adsorption properties of Pd adsorbed on MgO/Fe(001) and MgO(001) looked very similar to each other. The calculation results of Pd/MgO/Fe(001) showed that Pd binding decreases with the increase in the MgO film thickness and that the preferred site is on top of the surface O atom as in Pd/MgO(001). When the electronic structures were considered, however, the alignment of the energy levels was quite different. For Pd adsorbed on top of the surface O atom of MgO(001), the Pd $4d$ -derived states were formed in the gap region and the Fermi energy lay 1.3 eV above the top of the O valence band, whereas the Pd $5s$ -derived states were well separated from the Pd $4d$ -derived states and the energy difference was 1.1 eV [see Fig. 3(c)]. For Pd adsorbed at the surface O site on MgO/Fe(001), the Fermi energy lay 3.0 eV above the top of the O valence band. As a result, the

Pd 5s-derived state was partially filled and spin polarized [see Fig. 3(d)]. Here, the partial occupations of the Pd atoms could be understood as the probabilities of Pd to have Pd⁻ states over surface regions or in time. Our DFT-GGA calculations of Pd/MgO(3ML)/Fe(001) showed that almost half of Pd 5s states were occupied. This indicates that half of Pd atoms on surfaces or in time have Pd⁻ states. Figure 4(b) shows the isosurface plot of the electron-density difference $\Delta\rho$ for Pd/MgO(3ML)/Fe(001). Similarly to that of Au/MgO/Fe(001), substantial electron accumulation was found around Pd together with the polarization induction in the oxide [see Fig. 4(b)]. Our calculations clearly showed that the support-metal Fe helped negatively charge a metal atom even for Pd with a low EA. Interestingly, the Pd atom was also seen to be spin polarized with the presence of the Fe substrate. This charging spin-polarizing behavior is in sharp contrast to the neutral charge state of Pd or the negatively charged spin-unpolarized state of Au adsorbed on MgO/Mo(001).^{6,9} Considering that, when Pd atoms were negatively charged, they would have $d^{10}s^1$ configurations, leading to spin-polarized atoms. The spin polarization of Pd is basically an intrinsic property of Pd⁻ on MgO.

Further inspection revealed that the charge and/or spin states of Pd atoms on MgO/Fe(001) depend on the MgO film thickness. For Pd/MgO(1ML)/Fe(001), the Pd atom was nonmagnetic. Both the 5s spin-majority and spin-minority states of Pd were fully occupied, so the Pd atoms have Pd²⁻ states. When the MgO film thickness was increased to 2ML,

the ferromagnetic state of the Pd atom was favored, whereas the antiferromagnetic state was unstable. The 5s spin-majority state of Pd was fully occupied. With thicker Pd/MgO(3–5ML)/Fe(001), the weak magnetic interaction between the Pd atom and the substrate Fe was obtained. The 5s spin-majority state of Pd was in common found to be partially filled.²⁴

In summary, we have demonstrated that the Fe substrate supporting the MgO films significantly influences charge and/or spin states of TM atoms. Further analysis of MgO/Fe(001) showed that MgO overlayers induce decreases in work functions compared with that of Fe(001), as found in MgO/Mo(001) by Giordano *et al.*²⁵ For instance, for MgO(3ML)/Fe(001), the work function decreased from 4 to 2 eV. This provides a main driving force to the charge transfer from Fe to metal adsorbates. The present DFT-based results suggest Fe-supported ultrathin MgO films as a viable oxide model system for the study of charging or spin-polarizing effects on the chemical and the physical properties of metal atoms on ultrathin oxide films.

We thank Matthias Scheffler for valuable discussions. We also gratefully acknowledge support from the Korea Science and Engineering Foundation through the Basic Research Program under Grants No. R01-2004-000-10452 and No. R01-2007-000-20249 (B.D.Y.) and the Korea Research Foundation under Grant No. KRF-2008-314-C00132 (B.D.Y. and H.K.).

*Corresponding author; ybd@uos.ac.kr

¹H.-J. Freund, *Angew. Chem.* **109**, 444 (1997).

²C. Stampfl, M. V. Ganduglia-Pirovano, K. Reuter, and M. Scheffler, *Surf. Sci.* **500**, 368 (2002).

³M. S. Chen and D. W. Goodman, *Science* **306**, 252 (2004).

⁴M. S. Chen, Y. Cai, Z. Yan, and D. W. Goodman, *J. Am. Chem. Soc.* **128**, 6341 (2006).

⁵C. Freysoldt, P. Rinke, and M. Scheffler, *Phys. Rev. Lett.* **99**, 086101 (2007).

⁶G. Pacchioni, L. Giordano, and M. Baistrocchi, *Phys. Rev. Lett.* **94**, 226104 (2005).

⁷M. Sterrer, T. Risse, U. M. Pozzoni, L. Giordano, M. Heyde, H.-P. Rust, G. Pacchioni, and H.-J. Freund, *Phys. Rev. Lett.* **98**, 096107 (2007).

⁸H.-J. Freund, *Surf. Sci.* **601**, 1438 (2007).

⁹K. Honkala and H. Häkkinen, *J. Phys. Chem. C* **111**, 4319 (2007).

¹⁰V. Simic-Milosevic, M. Heyde, N. Nilius, T. König, H.-P. Rust, M. Sterrer, T. Risse, H.-J. Freund, L. Giordano, and G. Pacchioni, *J. Am. Chem. Soc.* **130**, 7814 (2008).

¹¹P. Hohenberg and W. Kohn, *Phys. Rev.* **136**, B864 (1964); W. Kohn and L. J. Sham, *ibid.* **140**, A1133 (1965).

¹²W. H. Butler, X.-G. Zhang, T. C. Schulthess, and J. M. MacLaren, *Phys. Rev. B* **63**, 054416 (2001).

¹³S. Yuasa, T. Nagahama, A. Fukushima, Y. Suzuki, and K. Ando,

Nature Mater. **3**, 868 (2004).

¹⁴T. Urano and Z. Kanaji, *J. Phys. Soc. Jpn.* **57**, 3403 (1988).

¹⁵M. Klaua, D. Ullmann, J. Barthel, W. Wulfhekkel, J. Kirschner, R. Urban, T. L. Monchesky, A. Enders, J. F. Cochran, and B. Heinrich, *Phys. Rev. B* **64**, 134411 (2001).

¹⁶H. Oh, S. B. Lee, J. Seo, H. G. Min, and J.-S. Kim, *Appl. Phys. Lett.* **82**, 361 (2003).

¹⁷B. D. Yu and J.-S. Kim, *Phys. Rev. B* **73**, 125408 (2006).

¹⁸J. P. Perdew, J. A. Chevary, S. H. Vosko, K. A. Jackson, M. R. Pederson, D. J. Singh, and C. Fiolhais, *Phys. Rev. B* **46**, 6671 (1992).

¹⁹D. Vanderbilt, *Phys. Rev. B* **41**, 7892 (1990).

²⁰G. Kresse and J. Hafner, *Phys. Rev. B* **47**, R558 (1993).

²¹G. Kresse and J. Hafner, *J. Phys.: Condens. Matter* **6**, 8245 (1994).

²²G. Kresse and J. Furthmüller, *Phys. Rev. B* **54**, 11169 (1996).

²³A. V. Matveev, K. M. Neyman, I. V. Yudanov, and N. Röscher, *Surf. Sci.* **426**, 123 (1999).

²⁴The partial filling of Pd 5s states was obtained within the DFT-GGA scheme. Possibly different computational approaches could give slight changes in level positions of Pd 5s states near the Fermi energy.

²⁵L. Giordano, F. Cinquini, and G. Pacchioni, *Phys. Rev. B* **73**, 045414 (2006).